arXiv:hep-ph/0312157v2 25 Jun 2004

IPPP/03/78
DCPT/03/156
DESY 03-203

Flavour in Intersecting Brane Models and Bounds on the String Scale

Steven A. Abel
IPPP, Centre for Particle Theory, University of Durham,
Durham DH1 3LE, UK

Oleg Lebedev
DESY Theory Group, D-22603 Hamburg, Germany

Jose Santiago
IPPP, Centre for Particle Theory, University of Durham,
Durham DH1 3LE, UK

1st February 2008

Abstract

We study flavour issues in nonsupersymmetric intersecting brane models. Specifically, the purpose of the present paper is twofold: (i) to determine whether realistic flavour structures can be obtained in these models, and (ii) to establish whether the non-supersymmetric models address the gauge hierarchy problem. To this end, we find that realistic flavour structures, although absent at tree level, can arise even in the simplest models after effects of 4 fermion instanton–induced operators and radiative corrections have been taken into account. On the other hand, our analysis of flavour changing neutral currents (FCNC), electric dipole moments (EDM), supernova SN1987A and other constraints shows that the string scale has to be rather high, 10^4 TeV. This implies that non-supersymmetric intersecting brane models face a severe finetuning problem. Finally, we comment on how non–trivial flavour structures can arise in supersymmetric models.

1 Introduction

Models with D-branes intersecting at angles [1] have received a great deal of attention due to their attractive phenomenological properties [2]- [17]. In particular, they have the potential to provide a nice geometric explanation of the fermion family replication (repeated generations correspond to multiple D-branes intersections), the Yukawa coupling hierarchy (Yukawa couplings depend exponentially on the area spanned by the brane intersections), and so on.

Since supersymmetric models arise only for specific values of intersection angles, realistic examples are relatively hard to come by, and many of the models that have been proposed are non-supersymmetric. Despite outstanding theoretical issues such as stability, non-supersymmetric configurations are interesting since they are a stringy realization of the ADD idea [18], with the string scale lying at just a few TeV. This requires that some of the compactified dimensions be large, which can be achieved in some brane constructions by, for instance, gluing a large volume manifold accessible to gravity only [11]. Thus, it seems possible that the gauge hierarchy problem can be addressed in non-supersymmetric models.

One known shortcoming of intersecting brane models comes from flavour physics, that is, the Yukawa matrices are predicted to be factorizable if the low energy theory is SM– or MSSM–like, e.g.

$$Y_{ij} = a_i b_j \ . \tag{1}$$

This is rank one and consequently only the third generation acquires mass. The result is not affected by field theory renormalization group running. One may therefore be tempted to dismiss such models at least as a way of generating a realistic fermion spectrum.

One of the purposes of this paper is to point out that there is always an additional source of flavour structures in non-supersymmetric intersecting brane models. This is the 4 fermion operators induced by string instantons. Their flavour structure is not the same as that of the Yukawa interactions in the sense that they cannot be diagonalized simultaneously. Through 1 loop threshold corrections (which are independent of the string scale), the 4 fermion operators contribute to the Yukawa couplings and destroy the factorizability of the Yukawa matrices. As a result, a realistic picture of the quark masses and mixings can emerge. It is important to emphasize that this mechanism applies to the *non-supersymmetric* models only due to SUSY non-renormalization theorems. For the supersymmetric case, we point out another plausible mechanism based on SUSY vertex corrections whose viability requires further study.

Another purpose of this paper is to determine whether intersecting brane models allow for a TeV string scale, for which we utilize the realistic flavour structures alluded to above. We employ the salient features of intersecting brane models, such as the mechanism for family replication, the presence of extra gauge bosons and so on, to obtain constraints on the string scale. The strongest bounds stem from the FCNC constraints which require the string scale to be no lower than $10^3 - 10^4$ TeV. Other considerations such as EDMs, supernova cooling, etc. allow for a lower string scale, $\mathcal{O}(10)$ TeV. Taken together, our results indicate that non-supersymmetric intersecting brane models suffer from a serious finetuning problem and the ADD idea cannot be realized. Supersymmetry or some other solution to fine-tuning is still required for realistic models. In particular, we note that the bound of 10^3 TeV applies for a whole host of independent flavour changing processes and it would be impossible to circumvent all of these bound by adjusting relevant parameters.

The issue of flavour physics constraints on the string scale was studied by two of us (S.A. and J.S.) in a previous publication [19]. That analysis could be (and indeed was) critisized in that there was not at the time a realistic model of flavour (due to the Yukawa factorization property) that could be used as a starting point. One might have argued that whatever mechanism eventually generates flavour also aligns contributions to the FCNC processes in such a way that they are suppressed. One of the points of the present work is to investigate whether such an alignment could occur. Here we find no evidence for it, and, on the contrary, establish that the bounds become significantly stronger than those presented in Ref. [19].

The fact that the FCNC constraints become stronger (compared to those of Ref. [19]) once the flavour model is specified is natural and can be explained as follows. The lower bound on the string scale in Ref. [19] was derived by varying the string scale as a function of the compactification scale. This was an *absolute* bound therefore: if we optimize the compactification scale to reduce FCNC, what is the minimum string scale that we can get away with? However, the compactification scales at the optimized compactification scale are typically not very realistic for gauge or Yukawa couplings because they are rather large, and large compactification scales tend to dilute the couplings with either large world volumes or large instanton actions. Hence, with a full model of flavour there is no longer any freedom to adjust compactification scales to reduce FCNC. The present work can be regarded as deriving the *typical* constraints in a realistic flavour model which, according to the argument above, should be stronger than the ones we obtained earlier.

In the following section, we begin by discussing contact interactions in intersecting brane models, and show that threshold effects can lead to a reasonable model of flavour. This 1–loop calculation will be done in a field theoretical manner, by using the flavour changing tree-level 4 point interaction (derived in string theory) as an effective vertex. In principle, a full string calculation of the threshold effects is possible as well [20] but this will be left to future work. Following this, we will derive the FCNC constraints and find that they are enhanced over the absolute bounds in Ref. [19]. We then turn to non–FCNC constraints, i.e. EDM, astrophysical, LEP consraints on contact interactions and constraints on the ρ parameter. In all cases, they are *subdominant*, and the FCNC constraints (in particular, those from the Kaon system, but also the B and D mesons)

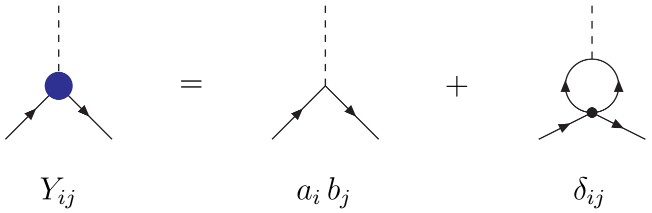

Figure 1: Threshold correction to Yukawa couplings. The black dot in the loop diagram represents a chirality changing four fermion amplitude.

are paramount. Nevertheless, they provide additional support for the statement that TeV–scale intersecting brane models are highly unlikely. It may be possible to fine-tune away one or a few undesirable effects, but it is surely impossible to fine-tune away all of them.

2 Realistic flavour structures from contact terms

In this section, we shall collect the components we need from the string theory calculations of amplitudes. In particular, as well as the tree-level Yukawa coupling interactions, we will need flavour structures to be introduced via four point couplings which are always present in this class of models. As we shall see, this naturally circumvents the "trivial Yukawa" (Eq.1) problem and provides a working model of flavour. The relevant diagram, shown in figure 1, generates a threshold correction to the Yukawa coupling structure. The blob in the loop diagram is the tree-level four fermion flavour changing coupling, coming with a factor of $1/M_S^2$, which can be calculated in string theory. The dimensionless Yukawa couplings get a significant (but loop–suppressed) contribution from this threshold correction if the effective cut-off in the loop momentum is similar to M_S, as is natural. In supersymmetric theories, there are two contributions, with fermions and bosons in the loop which cancel each other. In non–supersymmetric theories, this is not the case. For our purposes, it is sufficient to estimate this effect in field theory using a hard cut-off although a string theory calculation is also possible. (We shall discuss the procedure for performing the string calculation later.) What is important for us is that the threshold correction has a "nonfactorizable" form,

$$Y_{ij} = a_i b_j + \delta_{ij} \ . \tag{2}$$

Then, although the effect is loop–suppressed, it "redistributes" the large Yukawa coupling of the third generation and generates relatively small masses (as well as mixings) for the lighter generations.

The desired contact interactions also contribute to the flavour changing processes. However, their contributions are suppressed by a factor of $1/M_S^2$. Consequently, the FCNC effects decouple (unlike the threshold corrections) as the string scale is raised, and these interactions place a constraint of the string scale itself, as already seen in Ref. [19].

The contact interaction that will be of major importance is the four fermion interaction $(\overline{q}q)(\overline{q}q)$ which can in field theory be induced by a Higgs boson exchange. In string theory, these interactions can be much enhanced over the usual field theory amplitude suppressed by two Yukawa couplings. The key point can be summarized as follows. It is often assumed that, once the Yukawas have been determined from the non-perturbative "instanton" contribution, all other interactions can be understood perturbatively at the level of effective field theory. This assumption is incorrect if the string scale is low. In particular, for contact interactions generated by a Higgs boson exchange, in field theory, the amplitude is naturally proportional to the product of two Yukawa couplings. In string theory, this is not necessarily the case. As we shall see, the s- or t-channel Higgs exchange is extracted from the four fermion amplitude as a "double instanton" contribution (i.e. one instanton for each Yukawa coupling). However, the same 4 fermion operator may be generated by a single “irreducible” instanton, without going through the Higgs vertex. The corresponding amplitude will dominate if the single instanton action is significantly smaller than the double instanton action, i.e. if the area swept by propagating open strings is minimal for the former. This effect can be used to place strong constraints on M_S from observables such as electric dipole moments which are normally Yukawa–suppressed and plays a significant role in our discussion.

Let us now turn to the model. To be specific, we shall concentrate on the type of set-up shown in figure 2, first introduced in Ref. [21]. The gauge groups live on stacks of D6 branes, each of which wraps a 3 one-cycles in $T_2 \times T_2 \times T_2$. Although this set-up is not fully realistic, it captures all the features of the relevant contributions to FCNC and Yukawa couplings. More realistic configurations typically involve D5 and D4 branes (so that the transverse volumes can allow a low string scale without diluting the gauge couplings too much) and typically orientifolds. The effect of the latter is to introduce mirror branes. However, the interactions for strings that end on mirror branes are no different to those for strings on the original branes. At most, orientifolding changes gauge groups but makes no difference to the calculation of the 4 point couplings. What does change with orientifolding is the sums over contributions from multiply wrapped worldsheets. However, these contributions are exponentially suppressed and the calculation of leading terms is the same as that for flat non-compact space anyway. The situation with D4 and D5 branes can be trivially derived from the D6 brane case by simply switching off irrelevant contributions to the classical instanton action. (The quantum part generalizes easily but as we have said plays a minor role in this discussion.)

In the model of interest, we have four stacks of branes called baryonic (a), left (b),

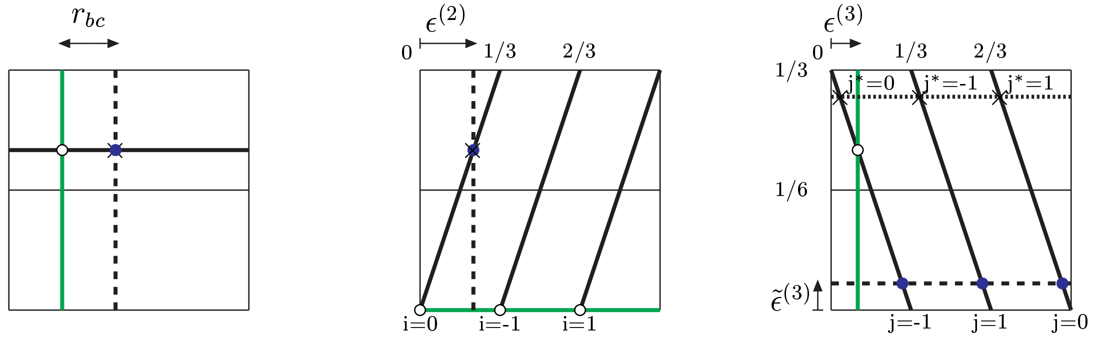

Figure 2: Brane configuration in a model of D6-branes intersecting at angles. The leptonic sector is not presented here while the baryonic, left, right branes and orientifold image of the right brane are the dark solid, faint solid, dashed and dotted lines, respectively. The intersections corresponding to the quark doublets ($i = -1, 0, 1$), up type singlets ($j = -1, 0, 1$) and down type singlets ($j^* = -1, 0, 1$) are denoted by an empty circle, full circle and a cross, respectively. All distances are measured in units of $2\pi R$ with R being the corresponding radius (except $\tilde{\epsilon}^{(3)}$ which is measured in units of $6\pi R$).

right (c) and leptonic (d), which give rise to the gauge groups $U(3) \sim SU(3) \times U(1)_a$, $SU(2)$ [1], $U(1)_c$ and $U(1)_d$, respectively. The matter fields live at the intersections of the branes and transform as the bi-fundamental representation of the corresponding groups, so that, for example, the open strings stretched between the U(3) brane and the SU(2) brane have (3,2) quantum numbers and hence are left handed quarks, the Higgs fields live at the intersection of the SU(2) and U(1) branes and so on. Yukawa couplings correspond to the emission of an open string mode at, say, the Higgs intersection which then travels to the opposing corners of a "Yukawa triangle". This is a non-perturbative process calculable with the help of conformal field theory techniques, as has recently been done in Refs. [22–24]. As one might expect, the amplitude is dominated by an exponential of the classical action. For 3 point (Yukawa) interactions, the action turns out to be equal to the sum of the areas of the triangles projected in each sub-torus. Thus,

$$Y \sim e^{-S_{cl}} \sim e^{-\sum_i \frac{\mathrm{Area}_i}{2\pi\alpha'}}$$

where $i = 1..3$ labels the 2-tori and α' is the string tension.

For the four (and higher) point couplings, there is no such prescription for extracting the contribution to the classical action, except for some simple cases [24]. Specifically, for an N-point function, only if the N-sided polygons in each sub-torus are either zero

---

[1] This particular model uses the orientifold projection to obtain the gauge group $USp(2) \sim SU(2)$ instead of the usual $U(2)$, see Ref. [21].

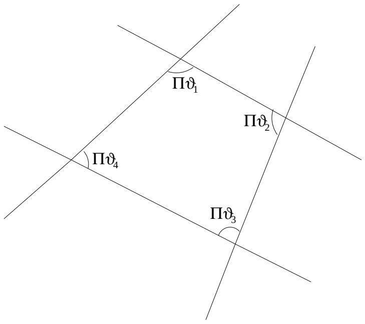

Figure 3: Generic 4 point string scattering diagram.

or the same (up to an overall scaling), is the classical action the sum of the projected areas. Otherwise factorizability is lost. We shall see this explicitly in the case of the four point functions. We will also observe that the 4 point diagram with a "Higgs intersection" reduces to the s- or t-channel Higgs exchange.

2.1 Generalities of the 4 point function calculation

In order to be completely general, we will consider the four fermion scattering amplitude in cases where independent branes intersect at arbitrary angles (bearing in mind that there can be three independent angles for $\bar{q}q\bar{l}l$ type diagrams). We need to determine the instanton contribution shown in figure 3. If the four intersecting branes form the boundary of a convex 4-sided polygon, with interior angles ϑ_i (in the units of π), then

$$\sum_{i=1}^{4} \vartheta_i = 2. \tag{3}$$

The leading contribution to the amplitude comes from the action with least area, which is the same in toroidal or planar cases. Due to our choice of the compactification manifold $T^2 \times T^2 \times T^2$, the amplitude can be factorized into a product of three contributions, one from each of the three sub-torus factors.

Denoting the spacetime coordinates for a particular sub-torus by $X = X^1 + iX^2$ and $\bar{X} = X^1 - iX^2$. The bosonic field X can be represented as a sum of a classical piece, X_{cl}, and a quantum fluctuation, X_{qu}. The amplitude then factorizes into classical and quantum components,

$$Z = \sum_{\langle X_{cl} \rangle} e^{-S_{cl}} Z_{qu}, \tag{4}$$

where

$$S_{cl} = \frac{1}{4\pi\alpha'} \int d^2 z \; (\partial X_{cl} \bar{\partial} \bar{X}_{cl} + \bar{\partial} X_{cl} \partial \bar{X}_{cl}). \tag{5}$$

Figure 4: t-channel Higgs exchange as a "double instanton".

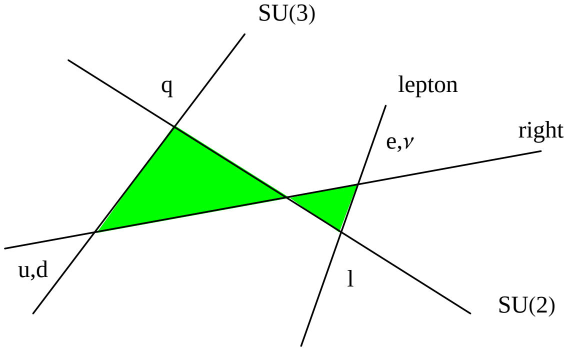

Here α' denotes the string tension. For our purposes, only the classical part of the amplitude, which takes account of the string instantons, is important. X_{cl} must satisfy the string equations of motion and possess the correct asymptotic behaviour near the polygon vertices (i.e. it has to "fit" in the vertex). The task of finding the solutions that meet these criteria forms a large part of the analyses in Refs. [22–24]. Having found the correct classical solutions X_{cl}, one then calculates the corresponding action. The Euclidian action leads to the well known area–suppression in the amplitude, as expected from instanton considerations.

A more detailed discussion of the calculation of the 4 point function are provided in the appendices. An important check is that the double instanton calculation agrees with the field theory result. In particular, the interaction $(\bar{u}u)(\bar{e}e)$ produced by combining the two Yukawa interactions as in Fig.4 goes as

$$\frac{Y_u Y_e}{t - M_H^2} \, ,$$

which is nothing but the field theory t-channel Higgs exchange, or the s-channel equivalent. However, as mentioned earlier, there are important stringy contributions to the same processes that have no field theory equivalent, and which are important sources of flavour changing. It is to these that we now turn.

2.2 Four point interactions and a model for Yukawa matrices

In string theory, some contact interactions can be generated without exchanging the Higgs. They are induced by a single instanton with no field theory pole (i.e. no brane intersection). It is important to note that such amplitudes can be significantly larger

Figure 5: "Irreducible" instanton contribution to 4 fermion operators.

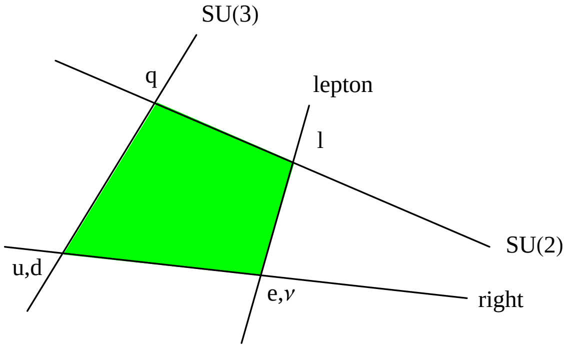

than the field theory contributions if the string scale is *low*. This is because the Higgs exchange involves the product of two Yukawa couplings. It is dominant if the leading diagram has one brane on either side of the intersection at which the Higgs is located. But if, for example, both the $SU(3)$ and lepton branes are lying on the same side of the Higgs intersection, as in Fig.(5), the contribution to $\bar{q}_L q_R \to \bar{e}_L e_R$ goes roughly as Y_e/Y_u and can be significantly enhanced for low string scales[2]. In the (unrealistic) limit that the lepton brane is lying on top of the SU(3) brane in all T_2 tori, there is no Yukawa suppression at all in this process. Note, however, that there should be an overall stringy suppression as there is no field theory limit and, therefore, no pole. Thus, one expects a contribution of the type

$$\frac{Y_e/Y_u}{M_S^2}\ .$$

Let us now consider the tree level Yukawa structure in the set-up of Fig.2. In this configuration, the generation number for the left–handed species varies in one of the T^2 sub-tori, while that for the right–handed species varies in some other sub-torus. We will refer to these tori as the "left" and "right" tori, respectively. Since the string action is a sum of the T^2–projected areas, the Yukawa coupling contains a factor that depends on the "left" generation number only and another factor depending on the "right" generation number,

$$(Y_q)_{ij} = a_i b_j\ . \tag{6}$$

This leads to two massless eigenstates, which is the "trivial Yukawa" problem alluded to earlier. Clearly, the contact interactions generated by a Higgs exchange are also factorizable since they are proportional to a product of the Yukawa couplings. However, generically the stringy 4 point couplings induce terms that do not factorize. This will be important for us since a nonfactorizable correction to a factorizable structure generally makes all of the eigenstates massive. This is in contrast to a factorizable correction, $(Y_q)_{ij} = a_i b_j + c_i d_j$, in which case one of the eigenstates remains massless (this is easily seen by noting that any vector orthogonal to b_j and d_j will be annihilated by Y_{ij}). In this case one would need an additional (third) correction of a different form. In fact, this situation occurs when the corrections to the Yukawa couplings are generated by the Kaluza–Klein mode exchange (which have a nontrivial flavour structure due to a generation–dependent coupling to KK modes of the gauge bosons [25]). Here we concentrate on the stringy instanton contributions in which case realistic flavour structures can be obtained.

---

[2] This is at the moment a heuristic argument; the Yukawa couplings are really matrices and, as we shall see, the generic 4 point instanton coupling does not simply reproduce an inverse Yukawa coupling.

Let us proceed by considering first a simple case when the relevant intersection quadrangle has a non–zero projection in one of the T^2 sub-tori only. By chirality considerations, in order to induce a correction to the Yukawa coupling, we need an operator of the type $(\overline{q}_{L_i} q_{R_j})(\overline{q}_{R_{j'}} q_{L_{i'}})$ in Fig.(6), which we discuss in more detail in Sec.4.3. The corresponding contribution to the $(\overline{q}_{L_i} q_{R_j})(\overline{q}_{R_{j'}} q_{L_{i'}})$ amplitude involves [24] (see also the appendices)

$$S_{cl} = \frac{1}{2\pi\alpha'} \left(\frac{\sin\pi\vartheta_1 \sin\pi\vartheta_4}{\sin(\pi\vartheta_1 + \pi\vartheta_4)} \frac{v_{14}^2}{2} + \frac{\sin\pi\vartheta_2 \sin\pi\vartheta_3}{\sin(\pi\vartheta_2 + \pi\vartheta_3)} \frac{v_{23}^2}{2} \right) . \tag{7}$$

Here ϑ_i are the angles and v_{14}, v_{23} are the sides of the quadrangle. Noting that $\sin(\pi\vartheta_2 + \pi\vartheta_3) = -\sin(\pi\vartheta_1 + \pi\vartheta_4)$, one may verify that this is simply the area/$2\pi\alpha'$ of the four–sided polygon. If the generation number i of the left–handed quarks varies in this sub-torus, while that of the right–handed quarks j varies in an orthogonal torus, the result is independent of j and the amplitude is proportional to $Y_{ij}/Y_{i'j} = a_i/a_{i'}$. This means that the 4 point function factorizes into a "left–handed" piece times a "right–handed" piece. Factorizability is also found in the "degenerate" case when the polygons in each T_2 torus are equivalent up to an overall scaling. This is because the action is again simply the sum of the projected areas.

In a more general situation, the classical action is no longer given by the sum of the projected areas. This is due to the presence of two conflicting contributions in the action such that its minimization does not produce a factorizable result. Consider the simplest non-trivial case, which is when the angles are the same for each sub-torus but the lengths v_{kl} differ. As we are interested in the operator $(\overline{q}_{L_i} q_{R_j})(\overline{q}_{R_{j'}} q_{L_{i'}})$, we have only two independent angles and $\vartheta_1 = 1 - \vartheta_2$ and $\vartheta_4 = 1 - \vartheta_3$. As we show in the appendices, the contribution to the coupling is dominated by a saddle point where the action in minimized. This gives [24]

$$S_{cl} = \frac{1}{4\pi\alpha'} \frac{\sin\pi\vartheta_2 \sin\pi\vartheta_3}{\sin(\pi\vartheta_2 + \pi\vartheta_3)} \sqrt{\sum_m (v_{23}^m - v_{14}^m)^2 \sum_n (v_{23}^n + v_{14}^n)^2} \ , \tag{8}$$

Figure 6: Chirality and flavour changing four fermion string amplitude. The corresponding polygons are generally *non–planar*, even for $i = l$. See also Fig.(2).

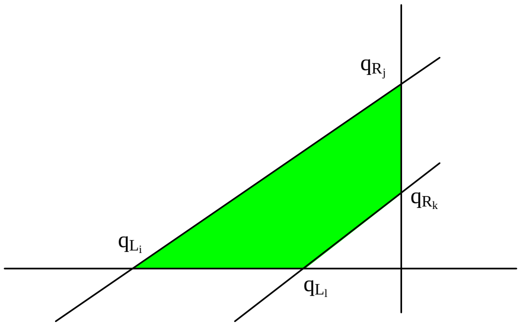

where m, n label the three sub-tori. Only for the trivial or degenerate cases described above does $e^{-S_{cl}}$ factorize into a "left–handed" and a "right–handed" pieces. This non–factorizability propagates into the Yukawa matrices through loop corrections.

Consider the model of Fig.2. For simplicity, we assume a common ratio of vertical to horizontal radii in the second and third tori: $R_2^{(2)}/R_1^{(2)} = R_2^{(3)}/R_1^{(3)} \equiv \chi$, where $R_{1,2}^{(I)}$ are the horizontal and vertical radii, respectively, of the $I-$th torus. The fact that the left and right branes are at right angles in the second and third tori and that the operator we are interested in is $(\bar{q}_{L_i} q_{R_j})(\bar{q}_{R_{j'}} q_{L_{i'}})$ leaves us with just one independent angle for all of the amplitudes, namely $\theta_{ab}^{(2)} = \frac{1}{2} - \theta_{ac}^{(2)} = \theta_{ac}^{(3)} = \frac{1}{2} - \theta_{ab}^{(3)} \equiv \sigma = \frac{1}{\pi}\tan^{-1}(3\chi)$. The location of the branes is parameterized by ϵ_2, ϵ_3 and $\tilde{\epsilon}_3$ as shown in Fig.2. There are two different types of diagrams that can contribute, depending on whether there is a crossing of the branes, so that the area swept out by propagating strings is formed by two triangles joined by the Higgs vertex, or there is no crossing, so that the relevant area is a convex four-sided polygon. If the areas in the two sub-tori are of the same kind, the corresponding action can be minimized analytically. For diagrams with a crossing, the result is proportional to the Yukawa couplings and no new flavour structure emerges. For diagrams without a crossing, the action is given by Eq.(8) and the corresponding correction to the Yukawa vertex is non–factorizable. The mixed case, crossing in one torus and non-crossing in the other, is more involved, depending on which sub–torus gives a dominant contribution to the action. If it is the non-crossing one, then the amplitude still factorizes, although it is no longer proportional to the Yukawa couplings (or the projected areas). It introduces new non-trivial, although factorizable, flavour structure. On the other hand, if the crossing diagram dominates, again a non-factorizable correction is found.

This new flavour structure appearing in the chirality changing four-fermion amplitude will propagate through radiative corrections to the Yukawa couplings. Using this amplitude as an effective vertex, we can estimate the one loop threshold correction to the Yukawa couplings, leading to a generic form

$$Y_{ij} \approx a_i b_j + \frac{\alpha}{\pi} A^{LR}_{ijkl} a_k b_l, \tag{9}$$

where A^{LR}_{ijkl} is the coefficient of the operator $\bar{q}_{L_i} q_{R_j} \bar{q}_{R_k} q_{L_l}$ and α/π represents a loop suppression.

This form ensures a natural hierarchy between the third and the first two families, with their masses generated at tree and one loop level, respectively. In order to get some intuition about the hierarchical structure of the first two families, it is useful to consider the limit in which the new contribution almost factorizes (recall that there are factorizable corrections that are not proportional to the Yukawa couplings) with a small non-factorizable correction

$$Y^{u,d}_{ij} = a_i b^{u,d}_j + \frac{\alpha}{\pi}\big(c_i d^{u,d}_j + \epsilon \tilde{C}^{u,d\ LR}_{ij}\big), \tag{10}$$

where ϵ measures departure from factorization in the chirality changing four-fermion amplitude. In the limit $\epsilon \to 0$, there is a massless state since there exists a 3D vector orthogonal to b_j and d_j and therefore annihilated by Y_{ij}. The matrices $Y^{u,d}_{ij}$ can be diagonalized perturbatively leading to the following values of the diagonal Yukawa couplings

$$Y^{u,d}_1 = \frac{\alpha}{\pi}\epsilon \mu^{u,d}_{11}, \quad Y^{u,d}_2 = \frac{\alpha}{\pi}\mu^{u,d}_1, \quad Y^{u,d}_3 = |a||b^{u,d}|, \tag{11}$$

and the mixings

$$\begin{aligned}
V^{CKM}_{12} =& \epsilon\Big[\frac{\mu^d_{12}}{\mu^d_1} - \frac{\mu^u_{12}}{\mu^u_1}\Big],\\
V^{CKM}_{13} =& \frac{\alpha}{\pi}\epsilon\frac{1}{|a|}\Big[\frac{\mu^u_{12}\mu^u_2/\mu^u_1 - \mu^u_{13}}{|b^u|} - \frac{\mu^u_{12}\mu^d_2/\mu^u_1 - \mu^d_{13}}{|b^d|}\Big],\\
V^{CKM}_{23} =& \frac{\alpha}{\pi}\frac{1}{|a|}\Big[\frac{\mu^d_2}{|b^d|} - \frac{\mu^u_2}{|b^u|}\Big].
\end{aligned}$$

Here $\mu^{u,d}_i$ and $\mu^{u,d}_{ij}$ are order one functions of a_i, b_i, c_i, d_i and $\tilde{C}^{LR}_{ij}$. The hierarchical pattern of quark masses and mixing angles found in nature [26]

$$\begin{aligned}
&m_u \sim 3\times 10^{-3}\ \text{GeV}, \quad m_c \sim 1.2\ \text{GeV}, \quad m_t \sim 174\ \text{GeV},\\
&m_d \sim 7\times 10^{-3}\ \text{GeV}, \quad m_s \sim 0.12\ \text{GeV}, \quad m_b \sim 4.2\ \text{GeV},\\
&V_{12} \sim 0.22, \quad V_{13} \sim 0.0035, \quad V_{23} \sim 0.04,
\end{aligned} \tag{12}$$

can be explained by a hierarchy in the expansion coefficients, α and ϵ. In fact, reasonable values for all experimental data in Eq.(12) can be obtained with

$$\frac{\alpha}{\pi} \sim 10^{-2}, \quad \epsilon \sim 0.1, \tag{13}$$

except for the up quark for which some amount of cancellation seems necessary.

In the model of Fig.2 things are a bit more involved, but a reasonable estimate can still be obtained. Keeping the ratio of the vertical to horizontal radii the same in the second and third tori (*i.e.* just one χ), the same $N = 1$ supersymmetry is preserved at all the intersections. In that case, the threshold correction from the four point amplitude vanishes due to non-renormalization theorems. As we shall see in the next sections, there are still sources of non-trivial Yukawa matrices even in that case. Consider now $\chi_2 \neq \chi_3$. The relevant parameters determining the flavour structure are then the horizontal radii of the second and third tori, $R_1^{(2,3)}$, the vertical to horizontal radii ratios, $\chi_{2,3}$ and the locations of the branes parameterized by ϵ_2, ϵ_3 and $\tilde{\epsilon}_3$ (see Fig. 2). Complex phases appear due to the Wilson lines or the antisymmetric backgroud field [21]. These are however irrelevant for the tree level Yukawa couplings since the factorization makes it possible to rephase them away. Non-trivial backgrounds also generate complex phases in the four-fermion amplitudes which then propagate through the threshold effects to the Yukawa couplings. We estimate their effects by adding random order one phases to the different entries of the amplitudes. The final parameter necessary to compute the quark masses is the ratio of the two Higgs VEVs, $\tan\beta$. For the following values of the parameters (dimensionful parameters are in string units)

$$\begin{aligned} &R_1^{(2)} = 1.1, \quad R_1^{(3)} = 1.15, \quad \chi_2 = 1.24, \quad \chi_3 = 0.94, \\ &\epsilon_2 = 0.121, \quad \epsilon_3 = 0.211, \quad \tilde{\epsilon}_3 = 0.068, \quad \tan\beta = 20, \end{aligned} \tag{14}$$

the spectrum of quark masses and mixing angles is reproduced with reasonable accuracy (recall a factor of a few uncertainty in the light quark masses):

$$\begin{aligned} &m_u \sim 4 \times 10^{-3}\ \text{GeV}, \quad m_c \sim 1.8\ \text{GeV}, \quad m_t \sim 176\ \text{GeV}, \\ &m_d \sim 4 \times 10^{-3}\ \text{GeV}, \quad m_s \sim 0.04\ \text{GeV}, \quad m_b \sim 8\ \text{GeV}, \\ &V_{12} \sim 0.22, \quad V_{13} \sim 0.003, \quad V_{23} \sim 0.02, \quad J = \mathcal{O}(10^{-5}), \end{aligned} \tag{15}$$

where we have included a global normalization factor 0.95 in the Yukawa couplings. Although the matching is not perfect, the point here is that a semirealistic pattern of fermion masses and mixing angles arises once the non-trivial flavour structure at one loop is taken into account. The rotation matrices defined by

$$L_{u,d}^{\dagger} Y_{u,d} R_{u,d} = Y_{u,d}^{\text{diag}} \tag{16}$$

take the following values:

$$|L_u| = \begin{pmatrix} 0.12 & 0.84 & 0.53 \\ 0.003 & 0.54 & 0.84 \\ 0.99 & 0.10 & 0.07 \end{pmatrix}, \quad \mathrm{Arg}(L_u) = \begin{pmatrix} -3.14 & 3.13 & -3.12 \\ -2.50 & -0.02 & -3.13 \\ 0 & \pi & \pi \end{pmatrix}, \tag{17}$$

$$|R_u| = \begin{pmatrix} 0.10 & 0.40 & 0.91 \\ 0.43 & 0.82 & 0.37 \\ 0.90 & 0.40 & 0.17 \end{pmatrix}, \quad \mathrm{Arg}(R_u) = \begin{pmatrix} -2.74 & -0.24 & -3.13 \\ 1.60 & 2.79 & -3.12 \\ -0.97 & -2.82 & -3.14 \end{pmatrix}, \tag{18}$$

$$|L_d| = \begin{pmatrix} 0.13 & 0.83 & 0.54 \\ 0.12 & 0.53 & 0.84 \\ 0.98 & 0.17 & 0.07 \end{pmatrix}, \quad \mathrm{Arg}(L_d) = \begin{pmatrix} -1.47 & 1.94 & -3.13 \\ 2.38 & -1.23 & -3.14 \\ 0 & 0 & \pi \end{pmatrix}, \tag{19}$$

and

$$|R_d| = \begin{pmatrix} 0.43 & 0.64 & 0.63 \\ 0.31 & 0.56 & 0.77 \\ 0.84 & 0.52 & 0.10 \end{pmatrix}, \quad \mathrm{Arg}(R_d) = \begin{pmatrix} 2.50 & 1.98 & -3.13 \\ -0.34 & -1.28 & -3.14 \\ -1.62 & 0.84 & -3.13 \end{pmatrix}. \tag{20}$$

These are the matrices we will use in the following sections to derive the FCNC bounds. Their effect (at least in our example) is non–trivial as they have significant off–diagonal entries and thus cannot be approximated by "a small angle" rotation matrix.

Finally, we note that if the low energy theory is described neither by the SM nor by the MSSM type model, non–trivial flavour structures can appear at tree level. For example, a model with 6 Higgs doublets has been studied in Ref. [27] and has been shown to generate a realistic spectrum.

2.3 One loop Yukawa thresholds in string theory

Here we have not attempted to calculate the 1–loop thresholds directly in string theory, which we defer until a subsequent publication. But there are a number of comments to make in this regard. In particular, it is interesting to see how the non-renormalization theorem appears in the string calculation.

The relevant diagrams are shown in figure 7. The annulus diagram has three vertex operators inserted on one boundary corresponding to the H, Q, U fields. These operators include bosonic twist fields whose job is to take the end of one string and move it from one brane to the next. The diagram therefore corresponds to the physical situation shown, where we have a string stretched between two branes. When we keep one end (B) fixed on some brane and move the opposing end (A) around the Yukawa triangle, we generate the three states appearing in the Yukawa coupling. The end (B) remains on the same brane and forms the inside edge of the annulus. It can be attached to any brane, although contributions from branes at large distance from the Yukawa

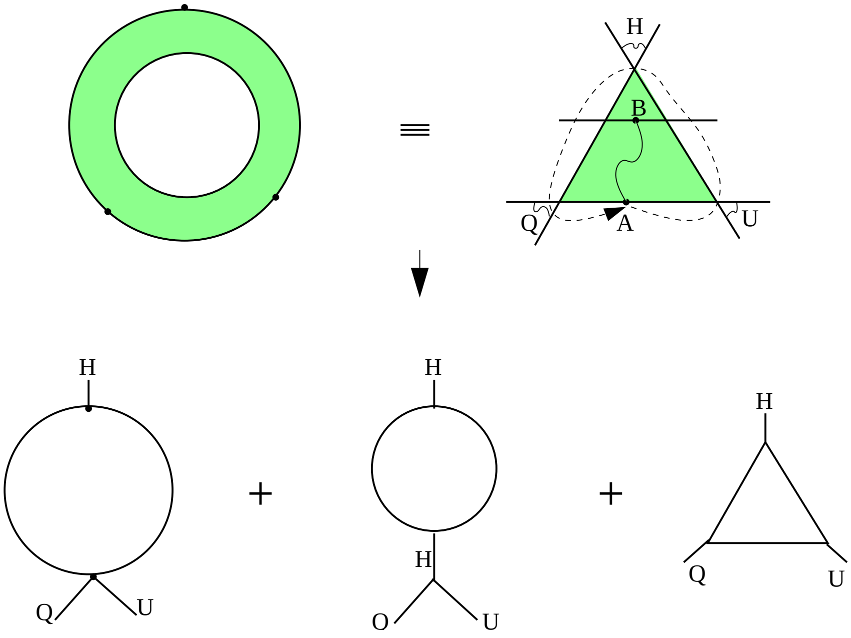

Figure 7: Threshold correction to Yukawa couplings in string theory. The string diagram is an annulus with three twist vertices on the external boundary. In the target space, the diagram corresponds to taking an open string stretched between two branes as shown, and moving one end around the Yukawa triangle. Various limits correspond to either the field theory threshold diagram with a four point operator inserted or the usual field theory renormalization diagrams. The wave function renormalization should be all that remains in supersymmetric configurations.

triangle are suppressed by instanton contributions. From a field theory point of view these would correspond to heavy stretched string states propagating in the loop. The diagram shows the case where end B is on the $SU(3)$ brane where the fields propagating in the loop are quarks and gluons. If B is on the $SU(2)$ brane, then the fields in the loop are the W boson, Higgs and left-handed quark. Note that the W boson is an "untwisted" state so that one would expect a sum over W Kaluza-Klein modes from these diagrams.

There are different field theory limits that one can take when evaluating the instanton action, which are also shown in the figure. Labelling the positions of the vertices on the boundary as x_H, x_Q, x_U, the one loop field theory diagrams shown are extracted in the limit $x_Q \to x_U$ (Note that only one of these is fixed by residual symmetry). We then have two possibilities. The first case corresponds to an instanton four point vertex and a Yukawa coupling. (The area swept out by the instanton world-sheet will be roughly the large triangle which is the sum of the small triangle and the four point area, so heuristically this makes sense. In $e^{-S_{cl}}$ we would expect to get a product of the two couplings.)

The second case occurs when the "A" endpoint travels through the Higgs intersection sweeping out three Yukawa triangles (or something approximating that). This corresponds to the standard Yukawa coupling renormalization.

The threshold contributions should decouple in supersymmetric theories, where only the field renormalization contributions are present by the non-renormalization theorem. The cancellation comes from a prefactor in the Yukawa couplings. The prefactor is found by factorizing the amplitude on the one loop partition function when all the vertices come together. In this limit one is left with the partition function on the annulus with ends on the two relevant branes. If these branes are tilted then supersymmetry can be completely broken, otherwise the prefactor vanishes by the "abstruse identity" if the branes are parallel. In this way we can see that in order to get a non-zero threshold in cases where the visible states preserve $N = 1$ supersymmetry, requires the interior of the annulus (end B) to be on a hidden brane. The threshold contributions will therefore come only from non-susy diagrams that involve states stretched between visible sector branes and the susy breaking hidden branes.

In the $N = 1$ case, one has to be a little more careful because not all contributions vanish, and those infra-red divergences that correspond to field renormalization should remain. This behaviour has to do with the Higgs pole term which is present for the field renormalization terms but not for the threshold terms. One expects (although this has to be checked) that the only non-vanishing contributions to these diagrams in supersymmetric theories are proportional to a factor $t - m^2$, so that, on mass-shell, the only non-vanishing pieces are those with a Higgs pole.

3 Remarks on flavour in supersymmetric models

We have shown that rich flavour structures arise in non–supersymmetric intersecting brane models at loop level. However, as we saw in the previous section, these arguments do not apply to globally supersymmetric models. This is due to non–renormalization of the N=1 superpotential which forces any threshold corrections to the Yukawa couplings to be suppressed by $m^2_{\rm SUSY}/M_S^2$, where $m_{\rm SUSY}$ is the soft breaking mass. The resulting quark masses are far too small. Also, we note that the brane intersection angles are fixed by supersymmetry, so there is less freedom in choosing the desired parameters.

Nevertheless, there is an additional source of flavour structures in supersymmetric models. In string theory, the soft breaking A–terms, although related to the Yukawas, generally have a different flavour pattern. This property is desirable from the phenomenological perspective and allows one to derive constraints on models of flavour and/or SUSY breaking [28]. Specifically, spontaneous breaking of supergravity requires [29]

$$A_{\alpha\beta\gamma} = F^m \left[\hat{K}_m + \partial_m \ln Y_{\alpha\beta\gamma} - \partial_m \ln(\tilde{K}_\alpha \tilde{K}_\beta \tilde{K}_\gamma)\right] . \tag{21}$$

Here the Latin indices refer to the "hidden sector" fields, while the Greek indices refer to the observable fields; the Kähler potential is expanded in observable fields as $K = \hat{K} + \tilde{K}_\alpha |C^\alpha|^2 + ...$ and $\hat{K}_m \equiv \partial_m \hat{K}$. The sum in m runs over SUSY breaking fields. The index convention is $Y_{H_1 Q_i D_j} \equiv Y^d_{ij}$ and so on. The soft trilinear parameters enter in the soft breaking Lagrangian as

$$\Delta\mathcal{L}_{\rm soft} = -\frac{1}{6} A_{\alpha\beta\gamma} Y_{\alpha\beta\gamma} C^\alpha C^\beta C^\gamma \, . \tag{22}$$

An analysis of SUSY soft breaking terms in intersecting brane models has recently been performed in [17].

What is important for us is that the A–terms are always flavour–dependent unless the moduli entering the Yukawa couplings do not break supersymmetry [28],

$$\Delta A_{ij} = F^m \partial_m \ln(a_i b_j) \, , \tag{23}$$

where $Y_{ij} = a_i b_j$. The Yukawa couplings depend, first of all, on the compactification radii, so the relevant moduli are the T–moduli. These generally break SUSY (unless a special Goldstino angle is realized). As a result, the soft breaking Lagrangian will contain a new flavour structure, not proportional to the original Yukawa matrices,

$$\Delta\mathcal{L}_{\rm soft} \sim {\rm const} \sum_{ij} a_i b_j (c_i + d_j) \; \tilde{q}^*_{L_i} \tilde{q}_{R_j} H + ... \tag{24}$$

The SUSY vertex corrections to the Yukawa interactions modify the tree level quark masses and mixings [30]. In particular, the gluino mediated diagram of Fig.8 generates a correction

$$Y_{ij} = a_i b_j + \epsilon \; a_i b_j (c_i + d_j) + ... \tag{25}$$

Figure 8: SUSY correction to the Yukawa coupling.

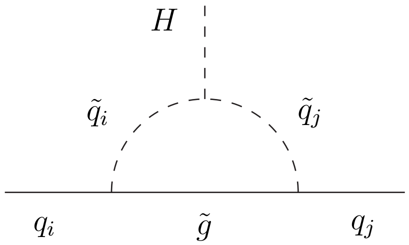

and analogously for the chargino and neutralino contributions. Note that this contribution does not decouple as the string scale or the soft breaking scale is raised. Here we have assumed universal masses for the sfermions in the loop. Corrections of this form induce masses for the second generation since there is only one 3D vector orthogonal to both b_j and $b_j d_j$ corresponding to a massless eigenstate. More sophisticated contributions (which include the RG running of the soft masses in the loop) can make all of the eigenstates massive. Whether this mechanism indeed leads to a realistic spectrum requires a separate study.

4 Constraints from flavour and CP physics

In this section, we analyze constraints on the string scale due to flavour and CP physics. The main point is that the mechanism of family replication in intersecting brane models leads to the existence of a large class of four fermion flavour and CP violating operators. These are suppressed by the string scale squared such that the experimental constraints can be interpreted as constraints on the string scale. In what follows, we first consider flavour violating processes and then turn to the flavour conserving CP–violating observables, the EDMs.

4.1 FCNC bounds

Instanton–induced 4 point amplitudes have allowed us to obtain a realistic pattern of fermion masses and mixing angles even in the simplest models with intersecting branes. They also contribute to *tree level* flavour violating transitions that are much suppressed in the Standard Model and extremely well constrained by experiment. Some of them (in particular, chirality conserving operators of Fig.9) along with FCNC generated by the exchange of gauge boson KK modes were considered in Ref. [19]. It was observed that the two sources of FCNC are *complementary* in their dependence on the compactification radii, such that an absolute bound $M_S \gtrsim 100$ TeV can be obtained independently

Figure 9: Chirality–preserving flavour changing string amplitude. See also Fig.(2).

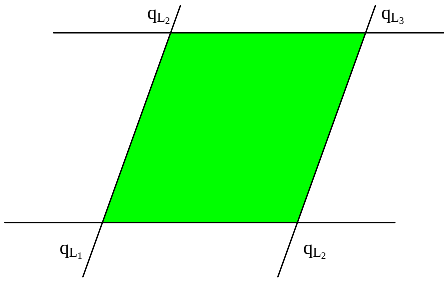

of the "size" of the extra dimensions. As we have emphasized in the introduction, this bound can only be treated as an estimate given the fact that a realistic theory of flavour was absent at that time. Now that we have one at our disposal we can make more reliable predictions in flavour physics and derive robust bounds on the string scale. Our mechanism of generating flavour structures fixes the compactification radii to be of order the string length because, in order to get enough flavour at one loop, the tree level Yukawa matrices must have relatively large entries. As a result, the bounds we obtain now are stronger than those derived previously.

It should be noted that the bounds from flavour physics generally depend on the flavour model. In particular, we have succeeded in generating realistic flavour structures from instanton–induced operators. One may also attempt to derive these from flavour–dependent quark couplings to the gauge KK modes which are important for large compactification radii. In this case the tree level Yukawa matrices are strongly hierarchical. We find that the corresponding flavour structures are quite restrictive and a realistic spectrum cannot be obtained (at least at one loop).

In this subsection, we discuss the most important flavour violating observables and the constraints they impose. We closely follow the analysis of Ref. [31], where a phenomenological study of models with a flavour non-universal extra U(1) was performed. The effect of the Z' exchange is mimicked by string instantons in our model. The four-fermion amplitudes are denoted by $A^{\chi_1\chi_2}_{ijkl}$, where $\chi_{1,2}$ are the chiralities of the amplitude and i, j, k, l are the generation indices. As the calculation is performed in the physical basis, we have to include the relevant rotation matrices. For instance, the "left-left" amplitude with four up type quarks reads

$$A^{LL}_{u_a u_b u_c u_d} = \sum_{ijkl} A^{LL}_{u_i u_j u_k u_l} (L_u^\dagger)_{ai} (L_u)_{jb} (L_u^\dagger)_{ck} (L_u)_{ld}, \tag{26}$$

where a, b, c, d are flavour indices and L_u is defined by (16). A similar expression holds for the other amplitudes.

We start our discussion with observables in the quark sector which we calculate using the rotation matrices (17). Leptonic and semileptonic observables will be *estimated* using rotation matrices with small angles.

4.1.1 Quark sector observables

The most constraining observables in the quark sector are those related to meson oscillations. In the SM, they are induced by one loop Cabibbo-suppressed box diagrams forcing them to be very small. The extreme experimental accuracy in oscillation measurements makes them an ideal place to constrain new flavour physics.

In our case, both the chirality preserving and chirality changing four-fermion amplitudes mediate meson oscillations at tree level. The mass splitting for a meson with quark content $P_0 = \bar{q}_j q_i$, in the vacuum insertion approximation, reads

$$\Delta m_P = \frac{2 m_P F_P^2}{M_S^2}\Big\{\frac{1}{3}\mathrm{Re}\big[A^{LL}_{ijij} + A^{RR}_{ijij}\big] - \Big[\frac{1}{2} + \frac{1}{3}\Big(\frac{m_P}{m_{q_i} + m_{q_j}}\Big)^2\Big]\mathrm{Re}A^{LR}_{ijij}\Big\}, \tag{27}$$

where m_P and F_P are the mass and decay constant of the meson, respectively. Here A_{ijkl} are the dimensionless coefficients parametrizing the 4f operators (with $1/M_S^2$ factored out).

Indirect CP violation in the Kaon system, which has been measured with extreme accuracy, is parametrized by

$$|\epsilon_K| = \frac{m_K F_K^2}{\sqrt{2}\Delta m_K M_S^2}\left|\Big\{\frac{1}{3}\mathrm{Im}\big[A^{LL}_{dsds} + A^{RR}_{dsds}\big] - \Big[\frac{1}{2} + \frac{1}{3}\Big(\frac{m_K}{m_d + m_s}\Big)^2\Big]\mathrm{Im}A^{LR}_{dsds}\Big\}\right|. \tag{28}$$

Numerically, the experimental constraints impose the following bounds:

- Kaon mass splitting

$$\frac{1}{M_S^2}\,\big|\mathrm{Re}\big[A^{LL}_{dsds} + A^{RR}_{dsds}\big] - 17.1\,\mathrm{Re}\big[A^{LR}_{dsds}\big]\big| \lesssim 3.3 \times 10^{-7}\ \mathrm{TeV}^{-2}, \tag{29}$$

- B mass splitting

$$\frac{1}{M_S^2}\,\big|\mathrm{Re}\big[A^{LL}_{dbdb} + A^{RR}_{dbdb}\big] - 3\,\mathrm{Re}\big[A^{LR}_{dbdb}\big]\big| \lesssim 2 \times 10^{-6}\ \mathrm{TeV}^{-2}, \tag{30}$$

- B_s mass splitting

$$\frac{1}{M_S^2}\,\big|\mathrm{Re}\big[A^{LL}_{sbsb} + A^{RR}_{sbsb}\big] - 3\,\mathrm{Re}\big[A^{LR}_{sbsb}\big]\big| \lesssim 6.6 \times 10^{-5}\ \mathrm{TeV}^{-2}, \tag{31}$$

- D mass splitting

$$\frac{1}{M_S^2}\,\big|\mathrm{Re}\big[A^{LL}_{ucuc} + A^{RR}_{ucuc}\big] - 3.9\,\mathrm{Re}\big[A^{LR}_{ucuc}\big]\big| \lesssim 3.3 \times 10^{-6}\ \mathrm{TeV}^{-2}, \tag{32}$$

- Kaon CP violation

$$\frac{1}{M_S^2}\left|\mathrm{Im}\big[A^{LL}_{dsds}+A^{RR}_{dsds}\big]-17.1\,\mathrm{Im}\big[A^{LR}_{dsds}\big]\right|\lesssim 2.6\times 10^{-9}\ \mathrm{TeV}^{-2}, \tag{33}$$

It is clear that if the coefficients of the 4 fermion operators are order one (times $1/M_S^2$), the Kaon system puts a constraint $M_S \gtrsim 10^{3-4}$ TeV. Later in this section we will use specific values of our rotation matrices to obtain more precise bounds.

4.1.2 (Semi) leptonic observables

We now turn to leptonic and semileptonic observables. Although some of them are very well determined experimentally, they only allow us to obtain a rough estimate of M_S since we do not properly address the issues of lepton flavour in this paper. The most constraining observables are the coherent $\mu - e$ conversion in atoms, heavy lepton decays and (semi)leptonic meson decays. Radiative lepton decays, such as $\mu \to e\gamma$, which are very important modes for some models of new physics (e.g. supersymmetry), are one loop transitions and, therefore, less restrictive than the tree level ones.

The expression for the new contribution to $\mu - e$ conversion is long and not very illuminating. Since we are only interested in an estimate, we consider the contribution of the left handed fields only. In that case, the muon conversion leads to the following constraint on the amplitude

$$\frac{1}{M_S^2}\left|A^{LL}_{e\mu uu}+1.1A^{LL}_{e\mu dd}\right|\leq 1.1\times 10^{-6}\ \mathrm{TeV}^{-2}, \tag{34}$$

which imposes a bound on M_S of roughly 10^{2-3} TeV.

Next, consider tau decays into three electrons or three muons. The contribution of the string instantons to the decay width is

$$\Gamma(l_j\to l_i l_i \bar{l}_l)=\frac{m_{l_j}^5}{384\pi^3 M_S^4}\Big(2\big|A^{LL}_{l_il_jl_il_i}\big|^2+2\big|A^{RR}_{l_il_jl_il_i}\big|^2+\big|A^{LR}_{l_il_jl_il_i}\big|^2+\big|A^{RL}_{l_il_jl_il_i}\big|^2\Big). \tag{35}$$

Using the experimental bounds on $\tau \to 3e$ and $\tau \to 3\mu$, respectively, we obtain the following constraints on the string amplitudes

$$\frac{1}{M_S^4}\Big\{\big|A^{LL}_{e\tau ee}\big|^2+0.78\big|A^{RR}_{e\tau ee}\big|^2+0.39\big|A^{LR}_{e\tau ee}\big|^2+0.5\big|A^{RL}_{e\tau ee}\big|^2\Big\}\leq 2.3\times 10^{-4}\ \mathrm{TeV}^{-4}, \tag{36}$$

and

$$\frac{1}{M_S^4}\Big\{\big|A^{LL}_{\mu\tau\mu\mu}\big|^2+0.78\big|A^{RR}_{\mu\tau\mu\mu}\big|^2+0.39\big|A^{LR}_{\mu\tau\mu\mu}\big|^2+0.5\big|A^{RL}_{\mu\tau\mu\mu}\big|^2\Big\}\leq 1.2\times 10^{-4}\ \mathrm{TeV}^{-4}. \tag{37}$$

These are inferior to the muon conversion constraints.

Flavour violating four fermion operators induce tree level corrections to leptonic and semileptonic decays of pseudoscalar mesons. The complete expressions are again long, complicated functions of the four-fermion coefficients, and in order to estimate the bounds we neglect the mixed LR contributions. Of the multitude of rare meson decays that have been measured, only the K_L^0 decays to two muons or two muons plus a pion are known with sufficient experimental precision to put strict bounds on new physics effects. The resulting constraints are

- $K_L^0 \to \mu^+\mu^-$

$$\frac{1}{M_S^2}\left|A^{LL}_{\mu\mu ds}+A^{LL}_{\mu\mu sd}+A^{RR}_{\mu\mu ds}+A^{RR}_{\mu\mu sd}\right| \leq 1.8\times 10^{-4}\mathrm{TeV}^{-2}, \qquad (38)$$

- $K_L^0 \to \pi^0\mu^+\mu^-$

$$\begin{aligned}\frac{1}{M_S^4}\Big\{0.75\Big[\big|A^{LL}_{\mu\mu ds}-A^{LL}_{\mu\mu sd}\big|^2+\big|A^{RR}_{\mu\mu ds}-A^{RR}_{\mu\mu sd}\big|^2\Big] & \qquad (39)\\ -0.48\mathrm{Re}\Big[\big(A^{LL}_{\mu\mu ds}-A^{LL}_{\mu\mu sd}\big)\big(A^{RR}_{\mu\mu ds}-A^{RR}_{\mu\mu sd}\big)^*\Big]\Big\} \quad \leq \quad & 2.1\times 10^{-8}\mathrm{TeV}^{-4}.\end{aligned}$$

Bounds of the order of 100 TeV are expected from these observables.

4.2 Numerical values

The above experimental constraints translate into bounds on the string scale once a model of flavour is chosen. The coefficients A_{ijkl} are then calculated in terms of the amplitudes in the original “flavour” basis and the rotation matrices L, R. In the lepton sector, the resulting bounds should be understood as rather naive estimates since we have not attempted to reproduce the observed lepton spectrum.

In any case, the consequent bounds are subleading. Regarding CP violation, we include random order one phases in the loop corrections (recall that the tree level phases can be rotated away). This makes the rotation matrices complex and results in a non–zero Jarlskog invariant. Using Eqs.(14) and (17,19), we obtain the bounds on the string scale shown in Table.1. The quark and leptonic observables are in the left and right columns, respectively. There are three features worth emphasizing. First, the bounds are extremely tight. This stems from *tree level* order one flavour violation with order one coupling constants. Second, the bounds one would naively expect are indeed realized which means that no unexpected cancellations are present. Finally, although (semi)leptonic observables are less restrictive, they provide an independent check such that it would be impossible to circumvent all of the above bounds.

Quark Observables	M_S (TeV)	(Semi)leptonic Observables	M_S (TeV)
Δm_K	1400	$\mu - e$ conversion	1000
Δm_B	800	$\tau \to 3e$	2
Δm_{B_s}	450	$\tau \to 3\mu$	2
Δm_D	1100	$K_L^0 \to \mu^+\mu^-$	260
$\lvert\epsilon_K\rvert$	4×10^4	$K_L^0 \to \pi^0\mu^+\mu^-$	300

Table 1: Bounds on the string scale from flavour violating observables.

4.3 Electric dipole moment bounds

In general, the four–fermion interactions induced by the string instantons violate CP as well as flavour conservation. CP violation in flavour changing processes has been considered above, but one also has constraints from flavour conserving observables such as the electric dipole moments.

The typical chirality–flipping 4–quark interactions contributing to the atomic and neutron EDMs (Fig.6) are of the form

$$\Delta\mathcal{L} = \mathcal{Y}_{ijkl}\ \bar{q}_L^i q_R^j \bar{q}_R^k q_L^l\ +\ \text{h.c.} \tag{40}$$

Here $\mathcal{Y}_{ijkl}$ is an instanton coupling which contains a complex phase (as do the Yukawa couplings) due to the presence of the antisymmetric background field and Wilson lines [3]. This coupling is suppressed by (roughly) the areas of the quadrangles spanned by the four vertices in each torus.

Let us first reiterate how relevant chirality flipping operators are generated. Some of the couplings $\mathcal{Y}_{ijkl}$ reduce to a product of the corresponding Yukawa couplings, i.e. when the "quadrangles" are formed by joining two $\bar{q}_L q_R H$ triangles through the Higgs vertex:

$$\bar{q}_L^i q_R^j H + \bar{q}_R^k q_L^l H^* \longrightarrow \bar{q}_L^i q_R^j \bar{q}_R^k q_L^l\ . \tag{41}$$

These "reducible" interactions are of no interest to us since they are real and flavour–diagonal in the basis where the quark mass matrix is diagonal. On the other hand, there exist "irreducible" contributions not mediated by the Higgs vertex, which are neither flavour–diagonal nor CP conserving in the physical basis. For example, some of these can be obtained (schematically) by combining the Yukawa interactions with the 4–quark chirality conserving operators $\bar{q}_L^i q_L^{i+1} \bar{q}_L^{k+1} q_L^k$ of Fig.9,

$$\bar{q}_L^{i+1} q_R^j H + \bar{q}_R^j q_L^{k+1} H^* + \bar{q}_L^i q_L^{i+1} \bar{q}_L^{k+1} q_L^k \longrightarrow \bar{q}_L^i q_R^j \bar{q}_R^j q_L^k\ . \tag{42}$$

---

[3] We note that this statement is not generic in string theory. Unlike in intersecting brane models, only the antisymmetric background field induces physical CP phases in heterotic string models [32].

Since the flavour structure of $\bar{q}^i_L q^{i+1}_L \bar{q}^{k+1}_L q^k_L$ is *independent* of that of the Yukawa matrices, the resulting interaction is not diagonal in the physical basis. To get a feeling for the strength of these interactions, it is instructive to consider a 2D case, i.e. when the couplings are given by the exponential of the relevant area. Then

$$\mathcal{Y}_{ijjk} \sim Y_{kj}/Y_{ij} \ . \tag{43}$$

This means that $\mathcal{Y}_{ijkl}$ are not necessarily suppressed by a product of the quark masses and can lead to significant constraints on the string scale.

Let us consider the down–type quark sector. The mass eigenstate basis is given by

$$d^i_L = L^{ij} (d_L)^j_{\rm mass} \ , \tag{44}$$

and similarly for the right–handed quarks. In what follows, we will drop the subscript "mass". The atomic/neutron EDM measurements constrain most severely operators of the type $\bar{d}_L d_R \bar{s}_R s_L$, $\bar{d}_L d_R \bar{b}_R b_L$, etc. Thus we are interested in

$$\begin{aligned} \Delta\mathcal{L} &= \left(\sum_{i,j,k,l} \mathcal{Y}_{ijkl} L^{i1*} R^{j1} R^{k2*} L^{l2} \right) \bar{d}_L d_R \bar{s}_R s_L \ + \ \text{h.c.} \\ &= \text{Im} C_{sd} \ (\bar{d} i\gamma_5 d \ \bar{s}s - \bar{s} i\gamma_5 s \ \bar{d}d) \ + \ (\text{CP} - \text{conserving piece}) \end{aligned} \tag{45}$$

and analogous terms with $s \rightarrow b$, etc. These CP violating operators contribute to the EDM of the mercury atom and the neutron [33]. The matrix element of the second operator in the parentheses over a nucleon is consistent with zero, while that of the first operator is known from low energy QCD theorems [34]. According to the recent analysis [35], the $d_{\rm Hg}$ bound requires

$$\text{Im} C_{sd} < 3 \times 10^{-11} \ \text{GeV}^{-2} \ . \tag{46}$$

The bound on $\text{Im}C_{bd}$ is about an order of magnitude weaker, while the constraint from d_n is less restrictive.

One can get a rough idea of how restrictive (46) is by considering a simple situation in which the rotation matrices L, R are similar to the CKM matrix. Then, an order of magnitude estimate gives

$$C_{sd} \sim \frac{1}{2} \mathcal{Y}_{1112} \ \sin\theta_C \ , \tag{47}$$

where $\mathcal{Y}_{1112}$ generally contains an order one phase and can be estimated using (43). In practice, when realistic L, R are used and many terms in C_{sd} are summed, cancellations suppress $\text{Im}C_{sd}$ by about an order of magnitude and the resulting bound is

$$M_S \gtrsim 10 \ \text{TeV} \ . \tag{48}$$

Although this bound is inferior to the FCNC bounds, it is still important as it implies that some finetuning is required to obtain a TeV- or 100 GeV-mass Higgs boson in non–supersymmetric models (recall that what matters is the square of the mass).

5 Supernovae and other constraints

In the previous sections we derived strong constraints on the string scale from flavour changing processes and electric dipole moments. We have utilized a salient feature of the intersecting brane models that there are 4 fermion flavor changing operators suppressed by M_S^2.

In this section, we will employ another rather generic feature of this class of models, namely, the presence of additional U(1) gauge bosons and light Dirac neutrinos. These additional U(1) symmetries are needed to protect a proton from decaying in models with a low string scale. Further, the intersecting brane constructions naturally lead to Dirac neutrinos since the neutrinos are localized at brane intersections and therefore are U(1) charged. The smallness of the neutrino masses is then explained by an exponential suppression of the relevant Yukawa couplings and a (relatively) large area of the triangle spanned by the Higgs, left lepton, and right neutrino vertices.

We will now use these generic features in order to obtain additional constraints on the string scale from non–FCNC experiments. We note that a bound on M_S of order 1 TeV from the electroweak ρ–parameter has previously been obtained in Ref. [36]. Below we will consider additional phenomenological constraints based on the presence of extra U(1) gauge bosons and Dirac neutrinos.

5.1 Supernova cooling

The first and potentially strongest constraint comes from the emission of the right handed neutrinos during supernova collapse, which affects the rate of supernova cooling [37]. This places a constraint on the 4 fermion axial vector interaction of the form

$$\mathcal{L}_R = \frac{4\pi}{\Lambda^2}\ \bar{q}\gamma_\mu\gamma_5 q\ \bar{\nu}_R\gamma^\mu\nu_R\ . \tag{49}$$

For 1 type of light Dirac neutrinos, the bound is [38]

$$\Lambda \gtrsim 200\ \text{TeV}\ , \tag{50}$$

where we have averaged over degenerate and non-degenerate nucleons. For 3 types of Dirac neutrinos the bound strengthens by a factor of $3^{1/4}$. A constraint on an analogous vector interaction is weaker ($\sim$ 90 TeV) since it leads to a coupling to the nucleon number (rather than the spin) density which does not fluctuate as much.

The interaction of the type (49) appears in intersecting brane models. Indeed, since the neutrinos are localized at the intersections of two branes, they are charged under two U(1)'s. The corresponding gauge bosons then mediate the contact quark–neutrino interaction. The strength of this interaction depends on two factors: the gauge boson masses and their couplings to fermions. These depend on the specifics of the model, yet the resulting lower bound on the string scale can be estimated quite well.

Let us consider the setup of Ref. [21]. In this case the so called *right* brane connects the right handed neutrinos and the right handed quarks. The corresponding "right" gauge boson mediates the interaction (49) at the tree level. Actually, to be exact, this gauge boson is not a mass eigenstate. The neutral gauge bosons of the model mix due to the Green–Schwarz mechanism. In particular, the neutral gauge boson mass matrix is given by

$$M_{ij}^2 = g_i g_j M_S^2 \sum_{a=1}^{3} c_a^i c_a^j \ , \tag{51}$$

where g_i is the gauge coupling of $\mathrm{U}(1)_i$, M_S is the string scale, and c_a^i couples the $\mathrm{U}(1)_i$ field strength to the RR two form field B_a (a=1,2,3) as $c_a^i B_a \wedge \mathrm{Tr} F^i$ and is fixed by the brane wrapping numbers. The gauge boson mass spectrum in intersecting brane models has been studied in Ref. [36]. It was found that the lightest mass eigenstate is lighter than the string scale (up to an order of magnitude), while the heaviest eigenstate is heavier than the string scale (up to two orders of magnitude). It was also found that the light states typically contain a significant component of the "right" or "leptonic" gauge bosons.

Further, to compute the contact interaction, one needs to know the couplings of the U(1) bosons to fermions. For the model of Ref. [21], the anomaly–free hypercharge is written as

$$q_{_Y} = \frac{1}{6} q_a - \frac{1}{2} q_c + \frac{1}{2} q_d \ , \tag{52}$$

where q_a is the charge associated with the U(3) color stack of branes, q_c – with the right brane, and q_d – with the leptonic brane. In general, if the charges are related by the transformation

$$q'_i = \sum_\alpha U_{i\alpha} q_\alpha \ , \tag{53}$$

the corresponding gauge couplings are related by

$$\frac{1}{g'^2_i} = \sum_\alpha \frac{U_{i\alpha}^2}{g_\alpha^2} \ . \tag{54}$$

Then, the gauge couplings g_c ("right") and g_d ("leptonic") are found via the relations

$$\begin{aligned} \frac{1}{g_Y^2} &= \frac{1}{36 g_a^2} + \frac{1}{4 g_c^2} + \frac{1}{4 g_d^2} \\ g_a^2 &= \frac{g_{QCD}^2}{6} \ . \end{aligned} \tag{55}$$

Figure 10: Tree level emission of right–handed neutrinos.

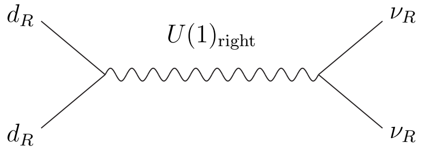

This means that g_c and g_d cannot be too small, and if one of them approaches its lower bound, the other one has to be rather large. Numerically, we have

$$\frac{1}{g_c^2} + \frac{1}{g_d^2} \sim 40 \,, \tag{56}$$

which implies that g_c and g_d are bounded from below by about 0.15.

Now we are ready to estimate the supernova bound on the string scale. Consider an exchange of a predominantly U$(1)_c$ gauge boson between d_R and ν_R (Fig.10). Neglecting the external momenta, the effective interaction is

$$\mathcal{L}_R = \frac{g_c^2}{2M_c^2} \; \bar{d}\gamma_\mu \gamma_5 d \; \bar{\nu}_R \gamma^\mu \nu_R \; + \; \text{vector piece} \,. \tag{57}$$

To get a conservative bound, set g_c to its minimal value ($\sim$0.15). Then we have $M_c \geq 5$ TeV. As the gauge bosons with a large U$(1)_c$ content are typically lighter than the string scale, this translates into a tighter bound on the string scale. On the other hand, the coupling of the light mass eigenstate to the quarks may be smaller than g_c if there is a significant U$(1)_d$ component. Assuming that these two effects roughly compensate each other, we get

$$M_S \gtrsim 5 \text{ TeV} \,. \tag{58}$$

In more realistic cases when g_c is larger than its minimal allowed value, the bound on the string scale lies in the range of tens of TeV (e.g. for $g_c \sim g_Y$, $M_S > 10$ TeV).

It is interesting to compare this leading tree level effect to the loop–induced quark–right neutrino coupling. It is generated by the mixing between the Z boson and the leptonic U$(1)_d$ gauge boson L via the diagram of Fig.11. This effect is also important because when the coupling g_c is suppressed, g_d is enhanced and the 1–loop contribution becomes considerable.

The origin of the Z–L mixing lies in the non–orthogonality of the Z– and the leptonic charges, which is an example of the "kinetic" mixing between U(1)'s [39] (see also recent work [40]). The induced interaction for the d–quarks is of the form

$$\mathcal{L}_R = \frac{g_Z^A g_d}{M_Z^2 M_L^2} \tilde{\Pi}_{ZL}(q^2=0) \; \bar{d}\gamma_\mu \gamma_5 d \; \bar{\nu}_R \gamma^\mu \nu_R \; + \; \text{vector piece} \,. \tag{59}$$

Figure 11: One loop emission of right–handed neutrinos.

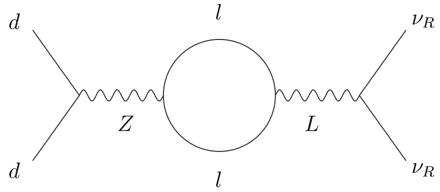

Here g_Z^A is the d–quark axial Z coupling and $\tilde{\Pi}_{ZL}(q^2 = 0)$ is the renormalized Z–L vacuum polarization at zero momentum transfer (again, L should be understood as a predominantly U(1)$_d$ gauge boson). We note that there is no similar mixing with the photon at zero momentum transfer by gauge invariance.

To find $\tilde{\Pi}_{ZL}$ we use the on–shell renormalization scheme for models with multiple U(1)'s of Ref. [41]. The renormalization conditions are imposed on the inverse gauge boson propagator in the Feynman gauge

$$\begin{aligned} D^{-1}_{\mu\nu}(q^2) &= i g_{\mu\nu} \begin{pmatrix} q^2 - M_Z^2 + \tilde{\Pi}_{ZZ}(q^2) & \tilde{\Pi}_{ZL}(q^2) \\ \tilde{\Pi}_{ZL}(q^2) & q^2 - M_L^2 + \tilde{\Pi}_{LL}(q^2) \end{pmatrix} \\ &= i g_{\mu\nu} \begin{pmatrix} D^{-1}_{ZZ} & D^{-1}_{ZL} \\ D^{-1}_{ZL} & D^{-1}_{LL} \end{pmatrix} , \end{aligned} \tag{60}$$

where we have omitted the $q_\mu q_\nu$ part of the vacuum polarization which would lead to the amplitude suppressed by the fermion masses. The six on–shell conditions read

$$\begin{aligned} D^{-1}_{ZZ}\Big|_{q^2=M_Z^2} = D^{-1}_{ZL}\Big|_{q^2=M_Z^2} = 0 \ , \quad \frac{\partial D^{-1}_{ZZ}}{\partial q^2}\Bigg|_{q^2=M_Z^2} = 1 \ , \\ D^{-1}_{LL}\Big|_{q^2=M_L^2} = D^{-1}_{ZL}\Big|_{q^2=M_L^2} = 0 \ , \quad \frac{\partial D^{-1}_{LL}}{\partial q^2}\Bigg|_{q^2=M_L^2} = 1 \ . \end{aligned} \tag{61}$$

They can be satisfied by choosing 3 appropriate "wave function" and 3 "mass" counterterms. The conditions for the off–diagonal propagator decouple form the others:

$$\tilde{\Pi}_{ZL}(M_Z^2) = \tilde{\Pi}_{ZL}(M_L^2) = 0 \ , \tag{62}$$

$$\tilde{\Pi}_{ZL}(q^2) = q^2 \Pi_{ZL}(q^2) + Z_{ZL} q^2 + \delta M_{ZL}^2 = \text{finite} \ , \tag{63}$$

where Z_{ZL} is the mixed "wave function" and δM_{ZL}^2 is the mixed "mass" counterterms (which do not enter into the diagonal conditions). As we are interested in $\tilde{\Pi}_{ZL}(0)$, we only need to compute δM_{ZL}^2.

The quantity $\Pi_{ZL}(q^2)$ is given by the bubble diagram with the Z and L external legs. It is actually identical to the one in QED (apart from the gauge couplings) due to the vectorial nature of the L boson. For one fermion in the loop and neglecting the lepton masses, we have

$$\Pi_{ZL}(q^2) = \frac{g_Z^V g_d}{6\pi^2}\left[\frac{1}{\epsilon} + c - \frac{1}{2}\ln\left(\frac{-q^2}{\mu^2}\right)\right] , \tag{64}$$

where g_Z^V is the vector Z coupling, $1/\epsilon + c$ is the UV part of the diagram, and μ is the renormalization scale. Solving (62) for δM^2_{ZL} and summing over all leptons, we get

$$\delta M^2_{ZL} = \left(\sum_\ell (g_Z^V)_\ell\right) g_d \; \frac{1}{12\pi^2}\frac{M_Z^2 M_L^2}{M_L^2 - M_Z^2}\ln\frac{M_Z^2}{M_L^2} \; . \tag{65}$$

Then the resulting quark–neutrino interaction can be written as

$$\mathcal{L}_R \simeq \frac{g^2 g_d^2 \tan^2\theta_W}{16\pi^2 M_L^2}\ln\frac{M_Z^2}{M_L^2}\; \bar{d}\gamma_\mu\gamma_5 d\; \bar{\nu}_R\gamma^\mu\nu_R \;+\; \text{vector piece} \; . \tag{66}$$

For $g_d \sim 0.2$ this places a bound on M_L of about 1 TeV, which according to the above arguments we can translate into

$$M_S \gtrsim 1 \text{ TeV} \; . \tag{67}$$

This result can be expected on general grounds since this bound is roughly a loop factor down compared to the tree level one.

Our conclusion here is that the supernova cooling constraint places a bound on the string scale of about 5 TeV at the tree level. If for some (special) reason the leading effect is suppressed, the loop induced amplitude constrains M_S to be above 1 TeV.

5.2 LEP constraints on contact interactions

The OPAL measurements of the angular distributions of the $e^+e^- \to \ell^+\ell^-$ processes [42] constrain the non–SM contact interactions of the type

$$\mathcal{L}_R = \frac{4\pi}{\Lambda^2}\; \bar{e}\gamma_\mu e\; \bar{\ell}\gamma^\mu\ell \; , \tag{68}$$

with

$$\Lambda > 9.3 \text{ TeV} \tag{69}$$

at 95% CL. Other types of contact interactions, i.e. axial, chirality specific, etc., are constrained slightly weaker. An exchange of the L gauge boson produces the vector–vector contact interaction above with $4\pi/\Lambda^2 = g_d^2/M_L^2$, which for $g_d \sim 0.2$ translates into

$$M_S \gtrsim 0.5 \text{ TeV} \; . \tag{70}$$

In most of the parameter space ($g_d > g_d^{\rm min}$), the bound is in the 1 TeV range. This is comparable to the 1σ bound from the ρ parameter obtained in Ref. [36].

5.3 ρ parameter.

This constraint has been studied in Ref. [36]. The basic idea here is that the physical Z boson has an admixture of "heavy" U(1) gauge bosons with Stückelberg masses. On the other hand, the W boson does not get a similar contribution. This modifies the Standard Model relation between the Z and W masses, i.e. affects the ρ–parameter

$$\rho = \frac{M_W^2}{M_Z^2 \cos^2 \theta_W} \ . \tag{71}$$

This leads to a (1σ) bound on the string scale in the range of 1 TeV,

$$M_S \gtrsim 1 \text{ TeV} \ . \tag{72}$$

There are further constraints similar in strength which rely on the presence of extra U(1) gauge bosons (see Ref. [43] for a comprehensive discussion).

6 Conclusions

In this work, we have studied the (related) issues of flavour and constraints on the string scale in intersecting brane models. Flavour is known to be a problematic point in these constructions. In particular, the Yukawa factorization property implies that the first two fermion families are massless and there is no quark mixing. In this paper, we pointed out that this is only true at tree level. The ever–present higher dimensional operators generated by string instantons contribute to the Yukawa couplings through one loop threshold corrections. As a result, the Yukawa factorizability is lost and realistic flavour structures are possible even in the simplest (non-supersymmetric) models. The lightness of the first two generations is then explained by the loop suppression. We note that this mechanism also fixes the relevant compactification radii to be around the string length.

Further, we addressed the issue of whether the string scale in intersecting brane models can be in the TeV range, as required in non–supersymmetric models. To answer this question, we employ generic features of this class of models such as the mechanism of fermion family replication, the presence of extra gauge bosons and Dirac neutrinos, etc. to obtain phenomenological constraints on the string scale. We found that the strongest bounds are due to the flavour changing neutral currents which appear at *tree* level. To suppress them sufficiently, the string scale has to be higher than 10^4 TeV. This bound has been derived using the flavour structure alluded to above, in which case the dominant FCNC contributions are induced by string instantons. In principle, if some compactification radii were relatively large, the dominant contribution would be provided by the gauge KK mode exchange and the bound on the string scale would relax to $\mathcal{O}(100)$ TeV [19]. However, it would be difficult (if possible at all) to obtain a realistic flavour pattern in this case.

Bounds on the string scale from other experiments are weaker. Nonobservation of the EDMs constrains CP–violating flavour–conserving operators, resulting in the bound $M_S > 10$ TeV (this bound is also sensitive to the model of flavour). Emission of right–handed neutrinos during supernova SN1987A collapse places a bound $M_S > 5-10$ TeV independently of the flavour model. Collider and ρ–parameter bounds are inferior, $M_S > 1$ TeV.

The above bounds are sufficiently strong to rule out a 1 TeV string scale. This allows us to conclude that non–supersymmetric intersecting brane models face a severe fine–tuning problem and supersymmetry is needed to address the hierarchy problem. We note that supersymmetry is also favoured by stability considerations.

It is not clear at the moment whether fully realistic flavour structures can arise in *supersymmetric* configurations. First of all, the intersection angles are more constrained. Also, due to the SUSY non–renormalization theorem, the threshold corrections to the Yukawa couplings from 4 point operators would behave as $m^2_{\rm SUSY}/M_S^2$ after SUSY breaking, which is too small to generate the light quark masses. Nevertheless, we point out that there is another source of flavour structures in SUSY models. The flavour pattern of the A–terms is different from that of the Yukawa matrices and the corresponding SUSY vertex corrections can generate non–zero masses for the light generations. Whether or not this mechanism produces a fully realistic spectrum remains to be seen.

Acknowledgements

It is a pleasure to thank I. Navarro and B. Schofield for useful discussions. This work was funded by PPARC and by Opportunity Grant PPA/T/S/ 1998/00833.

Appendices

A: The classical contribution to the amplitude

The equations of motion, asymptotic behaviour at intersections and monodromy conditions are sufficient to determine the classical instanton X_{cl} and its corresponding action. The action is expressed in terms of the hypergeometric functions

$$\begin{aligned} F_1 &= e^{-i\pi(\vartheta_2+\vartheta_3)} x_2^{-1+\vartheta_1+\vartheta_2} B(\vartheta_1,\vartheta_2)\,{}_2F_1(\vartheta_1, 1-\vartheta_3, \vartheta_1+\vartheta_2; x), \\ F_2 &= e^{-i\pi(-1+\vartheta_3)} (1-x_2)^{-1+\vartheta_2+\vartheta_3} B(\vartheta_2,\vartheta_3)\,{}_2F_1(\vartheta_3, 1-\vartheta_1, \vartheta_2+\vartheta_3; 1-x). \end{aligned} \tag{73}$$

We also define

$$\begin{aligned}
\alpha &= -\frac{\sin(\pi(\vartheta_1+\vartheta_2))}{\sin(\pi\vartheta_1)}, \\
\beta &= -\frac{\sin(\pi(\vartheta_2+\vartheta_3))}{\sin(\pi\vartheta_3)}, \\
\gamma &= \frac{\Gamma(1-\vartheta_2)\Gamma(1-\vartheta_4)}{\Gamma(\vartheta_1)\Gamma(\vartheta_3)}, \\
\gamma' &= \frac{\Gamma(\vartheta_2)\Gamma(\vartheta_4)}{\Gamma(1-\vartheta_1)\Gamma(1-\vartheta_3)},
\end{aligned} \tag{74}$$

and

$$\tau(x) = \left|\frac{F_2}{F_1}\right|. \tag{75}$$

The contribution to the action from a single sub-torus is found to be

$$S_{cl}^{T_2}(\tau, v_{21}, v_{32}) = \frac{\sin(\pi\vartheta_2)}{4\pi\alpha'}\left(\frac{((v_{21}\tau - v_{32})^2 + \gamma\gamma'(v_{21}(\beta+\tau) + v_{32}(1+\alpha\tau))^2)}{(\beta + 2\tau + \alpha\tau^2)}\right), \tag{76}$$

where v_{21} and v_{32} are the lengths of sides 12 and 23 in that particular subtorus. The complete expression for the classical action is just the sum of these contributions, one from each torus subfactor. Hence

$$S_{cl} = \sum_{m=1}^{3} S_{cl}^{T_2^m}(\tau^m, v_{21}^m, v_{32}^m). \tag{77}$$

The final amplitude (see below) involves an integration over x of the final expression which includes the factor $exp(-S_{cl}(x))$, and so is dominated by saddle point contributions given by (if the polygon is convex in all subtori)

$$\frac{\partial S_{cl}}{\partial x} = 0. \tag{78}$$

If the angles (and hence τ^m) are the same in every torus, we may easily get the saddle point using the condition

$$\frac{\partial S_{cl}}{\partial \tau} = 0 \tag{79}$$

instead, which has a simple functional form. In the case that the ratios of sides v_{12}^m/v_{23}^m are degenerate as well, the action reduces to the sum of the projected areas as in the 3 point case if the polygon is convex. However, this is a very special situation, and when it is not the case we find a source for new flavour structure.

B: The complete amplitude and s- and t-channel Higgs exchange

The above expressions together with the quantum piece may be used to determine any 4 point amplitude. Here, for the generation of a one-loop threshold contribution to the Yukawas, we will present the interactions that mimic Higgs exchange, with two left-handed and two right-handed fermions. First, we collect the quantum contributions to the amplitude. These are

$$\begin{aligned}
ghosts \times \langle e^{-\phi/2}(0) e^{-\phi/2}(x) e^{-\phi/2}(1) e^{-\phi/2}(x_\infty)\rangle &= x_\infty^{\frac{1}{2}} x^{-\frac{1}{4}}(1-x)^{-\frac{1}{4}}, \\
\langle e^{-ip_1.X} e^{-ip_2.X} e^{-ip_3.X} e^{-ip_4.X}\rangle &= x^{2\alpha' p_1.p_2}(1-x)^{2\alpha' p_2.p_3}, \\
\langle e^{iq_1.H} e^{iq_2.H} e^{iq_3.H} e^{iq_4.H}\rangle_{cmp} &= \prod_m^3 x_\infty^{\vartheta_4^m(1-\vartheta_4^m)-\frac{1}{4}} x^{\vartheta_1^m\vartheta_2^m-\frac{1}{2}(\vartheta_1^m+\vartheta_2^m)+\frac{1}{4}} \\
&\times\ (1-x)^{\vartheta_2^m\vartheta_3^m-\frac{1}{2}(\vartheta_2^m+\vartheta_3^m)+\frac{1}{4}}\ , \qquad (80)
\end{aligned}$$

where the last piece is for the three compactified tori factors only. The final piece comes from the uncompactified part of the fermions and is chirality dependent. We are interested in the operator $(\overline{q}_L^{(3)} q_R^{(2)})(\overline{e}_R^{(1)} e_L^{(4)})$ for which the uncompactified part of the fermions have charges (denoted $\tilde{q}_i$)

$$\begin{aligned}
\widetilde{q_1} &= -\tilde{q}_4 = \pm(\frac{1}{2},\frac{1}{2}), \\
\widetilde{q_2} &= -\tilde{q}_3 = \pm(\frac{1}{2},-\frac{1}{2}). \qquad (81)
\end{aligned}$$

Identifying the two ± possibilities with the Weyl spinor indices α of the fermions u_α, we see that in $\overline{u}_{\dot\alpha}^{(3)} \overline{u}_{\dot\beta}^{(2)} u_\gamma^{(1)} u_\delta^{(4)}$ we have opposite $\dot\alpha\dot\beta$ and $\gamma\delta$ indices which (writing as $\varepsilon_{\dot\alpha\dot\beta}\varepsilon_{\gamma\delta}$) just contract the $\overline{q}_L q_R$ and $\overline{e}_L e_R$ fermions. We then find

$$\begin{aligned}
\langle e^{-iq_1.H} e^{-iq_2.H} e^{-iq_3.H} e^{-iq_4.H}\rangle_{non-cmp} &= x_\infty^{\tilde{q}_4.(\tilde{q}_1+\tilde{q}_2+\tilde{q}_3)} x^{\tilde{q}_1.\tilde{q}_2}(1-x)^{\tilde{q}_2.\tilde{q}_3} \qquad (82) \\
&= x_\infty^{-\frac{1}{2}} x^{\tilde{q}_1.\tilde{q}_2}(1-x)^{\tilde{q}_2.\tilde{q}_3} = x_\infty^{-\frac{1}{2}}(1-x)^{-\frac{1}{2}}.
\end{aligned}$$

The additional half-integer power in the t-channel is required when we extract the Higgs pole in the $x \to 1$ limit.

Upon adding in the contribution from the bosonic twist fields as in Refs. [22]- [24], we find that dependence on ϑ_i^m cancels between the bosonic twist fields and the spin-twist fields. The final expression for the amplitude is (in four component notation)

$$\begin{aligned}
A(1,2,3,4) &= -g_s\alpha' \int_0^1 dx\ x^{-1-\alpha' s}(1-x)^{-1-\alpha' t} \frac{(1-x)^{-\frac{1}{2}}}{\prod_m^3 |J^m|^{1/2}} \\
&\times \left[(\overline{u}^{(3)}u^{(2)})(\overline{u}^{(1)}u^{(4)})\right] \sum e^{-S_{cl}(x)}\ . \qquad (83)
\end{aligned}$$

These amplitudes lead to the expected $s-$ and $t-$ channel Higgs exchanges. The Higgs field appears at the $SU(2)$-$U(1)$ brane intersection and so this process is the equivalent of the t-channel Higgs exchange in the field theory limit. The exchange appears as a double instanton as shown in figure 4 with the Higgs state appearing as a pole. The s-channel exchange corresponds to the opposite ordering of vertices (so $x \to 1-x$). Since the instanton suppression goes as $e^{-Area/2\pi\alpha'}$ we expect to find the product of two Yukawa couplings. The amplitude should go as

$$\frac{Y_u Y_e}{t - M_h^2}$$

or the s channel equivalent. We can verify this behaviour as follows.

It is easy to show that when the diagram has an intersection as in Fig.5, the action is monotonically decreasing and we may approximate the integral by taking the limit $x \to 1$. Assuming that $1 - \vartheta_2 - \vartheta_3 > 0$, the relevant limits are

$$\begin{aligned} Lim_{x\to 1}(\tau) &= -\beta \ , \\ Lim_{x\to 1}(J) &= (1-x)^{(-1+\vartheta_2+\vartheta_3)}\,\frac{1}{\gamma}\;\eta(\vartheta_2,\vartheta_3)\eta(1-\vartheta_1,1-\vartheta_4) \ , \end{aligned} \tag{84}$$

where

$$\eta(\vartheta_i,\vartheta_j) = \left(\frac{\Gamma(\vartheta_i)\Gamma(\vartheta_j)\Gamma(1-\vartheta_i-\vartheta_j)}{\Gamma(1-\vartheta_i)\Gamma(1-\vartheta_j)\Gamma(\vartheta_i+\vartheta_j)}\right)^{\frac{1}{2}} \ . \tag{85}$$

The normalization of the amplitudes and Yukawas can be obtained in this limit as in Ref. [22]. We take the limit where the 4 point function with no intersection turns into the 3 point function. The normalization factor for the general 4 point function is

$$2\pi \prod_{m=1}^{3} \sqrt{\frac{4\pi}{\gamma_m}\,\frac{\eta(1-\vartheta_2^m,1-\vartheta_3^m)}{\eta(\vartheta_1^m,\vartheta_4^m)}} \tag{86}$$

and the Yukawas take the form found in Ref. [22],

$$Y_{23}(A_m) = 16\pi^{\frac{5}{2}} \prod_{m}^{3} \eta(1-\vartheta_2^m,1-\vartheta_3^m) \sum_m e^{-A_m/2\pi\alpha'} \ , \tag{87}$$

where A_m is the projected area of the triangles in the m'th 2-torus. Once we add the intersection, the interior ϑ_1, ϑ_4 angles become exterior and should be replaced by $1-\vartheta_1$, $1-\vartheta_4$, respectively. The constraint on the interior angles is now $\vartheta_1+\vartheta_4 = \vartheta_2+\vartheta_3$ because of the intersection. Looking at $Lim_{x\to 1}(J)$ we see that this can be taken into account by adding an extra $\sqrt{\eta(1-\vartheta_1,1-\vartheta_4)/\eta(\vartheta_1,\vartheta_4)} = \eta(1-\vartheta_1,1-\vartheta_4)$ factor to the 4 point amplitude. We then find

$$S_4 = \alpha'\, Y_{23}(0)\, Y_{14}(0)\, e^{-S_{cl}(1)} \int_0^1 dx\,(1-x)^{-\alpha' t - \sum \frac{1}{2}(\vartheta_2^m+\vartheta_3^m)}. \tag{88}$$

The contribution to the classical action from each sub-torus becomes

$$S_{cl}(1) = \frac{1}{2\pi\alpha'}\left(\frac{\sin\pi\vartheta_1 \sin\pi\vartheta_4}{\sin(\pi\vartheta_1+\pi\vartheta_4)}\frac{v_{14}^2}{2} + \frac{\sin\pi\vartheta_2 \sin\pi\vartheta_3}{\sin(\pi\vartheta_2+\pi\vartheta_3)}\frac{v_{23}^2}{2}\right). \tag{89}$$

We see that the result is just the sum of the area/$2\pi\alpha'$ of the two triangles. Finally, the pole term now arises from the x integral,

$$\alpha' \int_0^1 dx\,(1-x)^{-\alpha' t - \sum \frac{1}{2}(\vartheta_2^m + \vartheta_3^m)} = \frac{1}{t - M_h^2}\ , \tag{90}$$

where (recalling that $0 < \vartheta_2^m + \vartheta_3^m < 1$) we recognize the mass of a scalar Higgs state in the spectrum at the intersection,

$$\alpha' M_h^2 = 1 - \frac{1}{2}\sum_m (\vartheta_2^m + \vartheta_3^m). \tag{91}$$

The opposite ordering of operators leads to the s- channel exchange in the $x \to 0$ limit. The above discussion was carried out for intersecting D6-branes, but it is straightforward to translate it to other set-ups.

References

[1] M. Berkooz, M. R. Douglas and R. G. Leigh, Nucl. Phys. B **480** (1996) 265 [arXiv:hep-th/9606139].

[2] R. Blumenhagen, L. Goerlich, B. Kors and D. Lust, JHEP **0010** (2000) 006 [arXiv:hep-th/0007024]; R. Blumenhagen, B. Kors and D. Lust, JHEP **0102** (2001) 030 [arXiv:hep-th/0012156]; R. Blumenhagen, B. Kors, D. Lust and T. Ott, Nucl. Phys. B **616** (2001) 3 [arXiv:hep-th/0107138].

[3] G. Aldazabal, S. Franco, L. E. Ibanez, R. Rabadan and A. M. Uranga, J. Math. Phys. **42** (2001) 3103 [arXiv:hep-th/0011073]; G. Aldazabal, S. Franco, L. E. Ibanez, R. Rabadan and A. M. Uranga, JHEP **0102** (2001) 047 [arXiv:hep-ph/0011132].

[4] L. E. Ibanez, F. Marchesano and R. Rabadan, JHEP **0111** (2001) 002 [arXiv:hep-th/0105155]; D. Bailin, G. V. Kraniotis and A. Love, Phys. Lett. B **530** (2002) 202 [arXiv:hep-th/0108131]; G. Honecker, JHEP **0201** (2002) 025 [arXiv:hep-th/0201037]; D. Cremades, L. E. Ibanez and F. Marchesano, JHEP **0207** (2002) 022 [arXiv:hep-th/0203160]; J. R. Ellis, P. Kanti and D. V. Nanopoulos, Nucl. Phys. B **647** (2002) 235 [arXiv:hep-th/0206087]; D. Bailin, G. V. Kraniotis and A. Love, Phys. Lett. B **547** (2002) 43 [arXiv:hep-th/0208103]; D. Bailin, G. V. Kraniotis and A. Love, Phys. Lett. B **553** (2003) 79 [arXiv:hep-th/0210219]; D. Bailin, G. V. Kraniotis and A. Love, arXiv:hep-th/0212112.

[5] R. Rabadan, Nucl. Phys. B **620** (2002) 152 [arXiv:hep-th/0107036].

[6] C. Kokorelis, arXiv:hep-th/0212281; arXiv:hep-th/0211091; JHEP **0209** (2002) 029 [arXiv:hep-th/0205147]; JHEP **0208** (2002) 018 [arXiv:hep-th/0203187]; arXiv:hep-th/0309070.

[7] D. Cremades, L. E. Ibanez and F. Marchesano, Nucl. Phys. B **643** (2002) 93 [arXiv:hep-th/0205074].

[8] R. Blumenhagen, L. Gorlich and B. Kors, JHEP **0001** (2000) 040 [arXiv:hep-th/9912204]; S. Forste, G. Honecker and R. Schreyer, Nucl. Phys. B **593** (2001) 127 [arXiv:hep-th/0008250]; M. Cvetic, G. Shiu and A. M. Uranga, Phys. Rev. Lett. **87** (2001) 201801 [arXiv:hep-th/0107143]; M. Cvetic, G. Shiu and A. M. Uranga, Nucl. Phys. B **615** (2001) 3 [arXiv:hep-th/0107166]; M. Cvetic, P. Langacker and G. Shiu, Nucl. Phys. B **642** (2002) 139 [arXiv:hep-th/0206115]; R. Blumenhagen, L. Gorlich and T. Ott, JHEP **0301** (2003) 021 [arXiv:hep-th/0211059]; M. Cvetic, I. Papadimitriou and G. Shiu, arXiv:hep-th/0212177; G. Honecker, arXiv:hep-th/0303015.

[9] M. Cvetic, P. Langacker and G. Shiu, Phys. Rev. D **66** (2002) 066004 [arXiv:hep-ph/0205252];

[10] D. Cremades, L. E. Ibanez and F. Marchesano, JHEP **0207** (2002) 009 [arXiv:hep-th/0201205].

[11] R. Blumenhagen, V. Braun, B. Kors and D. Lust, JHEP **0207** (2002) 026 [arXiv:hep-th/0206038]; A. M. Uranga, JHEP **0212** (2002) 058 [arXiv:hep-th/0208014].

[12] J. Garcia-Bellido, R. Rabadan and F. Zamora, JHEP **0201** (2002) 036 [arXiv:hep-th/0112147]; R. Blumenhagen, B. Kors, D. Lust and T. Ott, Nucl. Phys. B **641** (2002) 235 [arXiv:hep-th/0202124]; M. Gomez-Reino and I. Zavala, JHEP **0209** (2002) 020 [arXiv:hep-th/0207278].

[13] D. Lust and S. Stieberger, arXiv:hep-th/0302221.

[14] R. Blumenhagen, D. Lust and T. R. Taylor, arXiv:hep-th/0303016; J. F. Cascales and A. M. Uranga, arXiv:hep-th/0303024.

[15] R. Blumenhagen, D. Lust and S. Stieberger, JHEP **0307** (2003) 036 [arXiv:hep-th/0305146].

[16] M. Axenides, E. Floratos and C. Kokorelis, JHEP **0310** (2003) 006 [arXiv:hep-th/0307255].

[17] B. Kors and P. Nath, arXiv:hep-th/0309167.

[18] N. Arkani-Hamed, S. Dimopoulos and G. R. Dvali, Phys. Lett. B **429**, 263 (1998) [arXiv:hep-ph/9803315]; I. Antoniadis, N. Arkani-Hamed, S. Dimopoulos and G. R. Dvali, Phys. Lett. B **436**, 257 (1998) [arXiv:hep-ph/9804398].

[19] S. A. Abel, M. Masip and J. Santiago, JHEP **0304** (2003) 057 [arXiv:hep-ph/0303087].

[20] Abel, Schofield, in preparation.

[21] D. Cremades, L. E. Ibanez and F. Marchesano, "Towards a theory of quark masses, mixings and CP-violation," arXiv:hep-ph/0212064; D. Cremades, L. E. Ibanez and F. Marchesano, JHEP **0307**, 038 (2003).

[22] M. Cvetic and I. Papadimitriou, Phys. Rev. D **68** (2003) 046001 [arXiv:hep-th/0303083].

[23] S. A. Abel and A. W. Owen, Nucl. Phys. B **663** (2003) 197 [arXiv:hep-th/0303124].

[24] S. A. Abel and A. W. Owen, arXiv:hep-th/0310257.

[25] C. D. Carone, Phys. Rev. D **61**, 015008 (2000).

[26] K. Hagiwara et al., Phys. Rev. **D66**, 010001 (2002)

[27] N. Chamoun, S. Khalil and E. Lashin, arXiv:hep-ph/0309169.

[28] S. Abel, S. Khalil and O. Lebedev, Phys. Rev. Lett. **89**, 121601 (2002).

[29] S. K. Soni and H. A. Weldon, Phys. Lett. B **126**, 215 (1983); V. S. Kaplunovsky and J. Louis, Phys. Lett. B **306**, 269 (1993).

[30] R. Hempfling, Phys. Rev. D **49**, 6168 (1994); L. J. Hall, R. Rattazzi and U. Sarid, Phys. Rev. D **50**, 7048 (1994).
For applications to flavour physics see, e.g., J. L. Diaz-Cruz, H. Murayama and A. Pierce, Phys. Rev. D **65**, 075011 (2002); D. A. Demir, Phys. Lett. B **571**, 193 (2003).

[31] P. Langacker and M. Plumacher, Phys. Rev. D **62** (2000) 013006 [arXiv:hep-ph/0001204].

[32] T. Kobayashi and O. Lebedev, Phys. Lett. B **565**, 193 (2003); Phys. Lett. B **566**, 164 (2003).

[33] I. B. Khriplovich and S. K. Lamoreaux, "CP Violation Without Strangeness: Electric Dipole Moments Of Particles, Atoms, And Molecules," Springer, 1997.

[34] M. A. Shifman, A. I. Vainshtein and V. I. Zakharov, Phys. Lett. B **78**, 443 (1978).

[35] D. Demir, O. Lebedev, K. Olive, M. Pospelov, A. Ritz, hep-ph/0311314; O. Lebedev and M. Pospelov, Phys. Rev. Lett. **89**, 101801 (2002).

[36] D. M. Ghilencea, L. E. Ibanez, N. Irges and F. Quevedo, JHEP **0208**, 016 (2002); D. M. Ghilencea, Nucl. Phys. B **648**, 215 (2003).

[37] G. Raffelt and D. Seckel, Phys. Rev. Lett. **60**, 1793 (1988).

[38] J. A. Grifols, E. Masso and R. Toldra, Phys. Rev. D **57**, 2005 (1998).

[39] B. Holdom, Phys. Lett. B **166**, 196 (1986).

[40] K. R. Dienes, C. F. Kolda and J. March-Russell, Nucl. Phys. B **492**, 104 (1997); W. Loinaz and T. Takeuchi, Phys. Rev. D **60**, 115008 (1999); L. N. Chang, O. Lebedev, W. Loinaz and T. Takeuchi, Phys. Rev. D **63**, 074013 (2001); S. A. Abel and B. W. Schofield, arXiv:hep-th/0311051.

[41] F. del Aguila, M. Masip and M. Perez-Victoria, Nucl. Phys. B **456**, 531 (1995).

[42] G. Abbiendi *et al.* [OPAL Collaboration], Eur. Phys. J. C **6**, 1 (1999).

[43] A. Leike, Phys. Rept. **317**, 143 (1999); M. Cvetic and P. Langacker, "Z' physics and supersymmetry," arXiv:hep-ph/9707451.